SF2A 2024
M. Béthermin, K. Baillié, N. Lagarde, J. Malzac, R.-M. Ouazzani, J. Richard, O. Venot, A. Siebert (eds)

PREDICTING THE DETECTABILITY OF SULFUR-BEARING MOLECULES IN THE SOLID PHASE WITH SIMULATED SPECTRA OF JWST INSTRUMENTS

A. Taillard[1], R. Martin-Domenech[1], H. Carrascosa[1], G. M. Munoz Caro[1], J. A. Noble[2], E. Dartois[3], D. Navarro-Almaida[4], A. Sanchez-Monge[5,6] and A. Fuente[1]

Abstract. In star forming regions, S-bearing species in the gas-phase (SO, SO_2, CS, HCS^+, C_2S and C_3S) represent only a fraction (<1%) of the cosmic sulfur abundance. We expect that most of the sulfur in the interstellar medium (ISM) is locked within the solid-phase, whether in ice mantles or in the (semi-)refractory material. The search for solid sulfur in the ISM is still elusive: only OCS has been solidly detected and SO_2 tentatively detected. Yet, the estimated column densities of these two molecules would only represent about 5% of the cosmic sulfur abundance, leading to more than 90% still hidden within a non-identified form.

Chemical models struggle to implement the sulfur chemistry as compared to other elements, despite recent efforts to update the chemical networks. Models predict that a large fraction of the S-bearing volatile species in dense cores is within the ice mantle, but identifying a unique reservoir is no easy task: most of these species are highly dependent on the physical conditions and chemical age of the cloud. Recent observations suggest that the sulfur depletion and S-bearing species distribution in ices is strongly affected by the dynamical and chemical history of the cloud, leading to very different ice compositions.

In this work, we update CS_2 band parameters and present for the first time the near-infrared (IR) S_8 spectrum. We then present a synthetic IR ice spectra generator based on the James Webb Space Telescope (JWST) instrumentation and built around a simple approximation from laboratory spectra. This tool is used to study the detectability of S-bearing species (in particular H_2S, CS_2, SO_2 and S_8) in ice mantles within the JWST wavelength range (0.6-28.3 μm). Multiple flat continuum of different intensities are tested to derive the column densities needed to reach a 5σ detection for each species within three different scenarios (dense cloud, LYSO and MYSO).

We conclude that the detection of the selected S-bearing species is challenged by the ice composition and ice processing in different environments, suggesting that solid sulfur might remain hidden from us.

Keywords: Astrochemistry, Infrared: ISM, solid state: volatile

1 Introduction

Sulfur is the tenth most abundant element in the Universe (Asplund et al. 2009) and is believed to play an important role in the chemistry of star forming regions. In the gas-phase, atomic S is the main atomic electron donor at low Av (3.7 - 7 mag), regulating the gas ionisation fraction (Fuente et al. 2023). On surfaces, small S-bearing molecules, such as H_2S, play a catalyst role in the formation of complex molecules (Moore et al. 2007). However, despite recent observational efforts, it is estimated that the S-bearing species, both in gas- and solid-phase, only represents about 5% of the total sulfur cosmic abundance (assuming S/H $\sim 1.5 \times 10^{-5}$ in diffuse cloud mainly in the form of S^+, Jenkins 2009). In prestellar cores, multiple S-bearing molecules have been identified (mainly SO, SO_2, CS, HCS^+, H_2CS, C_2S and C_3S) but only account for $< 1\%$ of the cosmic abundance (Agúndez & Wakelam 2013; Vastel et al. 2018). While in the solid-phase, only the 4.9 μm feature in

[1] Centro de Astrobiología (CAB), CSIC-INTA, Ctra. de Ajalvir, km 4, Torrejón de Ardoz, 28850 Madrid, Spain
[2] Physique des Interactions Ioniques et Moléculaires, CNRS, Aix Marseille Univ., 13397 Marseille, France
[3] Institut des Sciences Moléculaires d'Orsay, CNRS, Univ. Paris-Saclay, 91405 Orsay, France
[4] Université Paris-Saclay, Université Paris Cité, CEA, CNRS, AIM, F-91191 Gif-sur-Yvette, France
[5] Institut de Ciències de l'Espai (ICE, CSIC), Campus UAB, Carrer de Can Magrans s/n, 08193, Bellaterra (Barcelona), Spain
[6] Institut d'Estudis Espacials de Catalunya (IEEC), 08860 Castelldefels (Barcelona), Spain

the IR spectrum has been associated to OCS (C-S stretching) toward background stars (McClure et al. 2023), embedded objects (Palumbo et al. 1995), protostar (Palumbo et al. 1997), class 0-I (Gibb et al. 2004; Aikawa et al. 2012) and MYSO (Boogert et al. 2022). SO_2 possible feature at 7.7 μm has been classified as "likely" in a recent study (Rocha et al. 2023), towards a low-mass class 0 protostar and a high-mass protostar. So far, no other S-bearing molecules has been identified in ISM ices. From *in situ* observations of the coma of comet 67P/Churyumov-Gersimenko (Calmonte et al. 2016), atomic S, H_2S, SO_2, OCS and SO were identified, suggesting that these species could already be present in the cold regions of the ISM. Additionally, Calmonte et al. (2016) inferred the presence of S_3^+ and S_4^+ in the coma, introducing the possibility that the sulfur might be locked in S-allotropes, also supported by ab initio calculations and lab experiments (Cazaux et al. 2022).

Since we are lacking observational constraints, the non-detection of S-bearing species challenges the astrochemical models, where multiple problems were highlighted and partially corrected in Vidal et al. (2017). Recent modelling efforts, such as Laas & Caselli (2019) and Navarro-Almaida et al. (2020) have been trying to identify the main sulfur reservoirs in the solid-phase, but show that the ice composition and exact main carrier of these species is highly dependent on the physical conditions. Overall, the models agree that most of the sulfur (> 99%) is depleted into the grain (ices and (semi-)refractories) in cold molecular regions. The comparison between observations and models is however very limited.

Considering the available observations, modelling results and laboratory experiments, we identified several S-bearing species to be searched for in the ices (H_2S, OCS, SO_2, CS_2, S-allotropes), thanks to the better sensitivity and better spectral resolution offered by the JWST instruments, NIRSpec and MIRI. To do so, we use the Synthetic Ice Spectrum generator (SynthIceSpec, Taillard et al, in prep) to test the detectability of these S-carriers in different objects (dense cloud, LYSO and MYSO), supported by new laboratory data and chemical modelling results.

2 CS_2 and S_8 band parameters

In order to look for the different S-carriers, we need their vibrational modes band parameters, ideally found in the JWST wavelength range (0.6-28.3 μm). For this study, we were lacking CS_2 and S_8 data. We carried an experiment in a ultra high-vacuum chamber where we deposited a CS_2 ice sample on a CsI substrate at 8 K using the SPACE TIGER experimental setup at the Center for Astrophysics (CfA, Harvard & Smithsonian, USA). With the new spectrum, we computed the band strength and width of the main feature knowing the approximate CS_2 column densities deposited on the sample. The band strength was estimated at 1.3×10^{-16} cm^{-1} for the 6.6 μm feature. We also made an estimation of the band strength of the S_8 main feature at 21.3 μm. The experiment was carried out at the Centro de Astrobiología (CAB, CSIC-INTA, Spain), where a S_8 pellet was introduced in a Fourier-Transform IR spectrometer, resulting of a band strength of 1.5×10^{-19} cm^{-1}.

3 SynthIceSpec

To test the detectability of the selected species, we used a synthetic ice generator (SynthIceSpec, Taillard et al, in prep.) to derive iteratively the needed column densities to obtain a 5σ detection. The code uses a simple approximation that the molecular vibrational band can be reproduced by a Gaussian or a sum of Gaussian. The optical depth is obtained by multiplying the assumed column density by the band strength, integrated under the distribution profile with a given full width half maximum (bandwidth). The code takes in consideration the different JWST instrumental parameters (spectral resolution, wavelength range...) and we add a synthetic noise all over the spectrum, extracted from actual data published in (McClure et al. 2023). The absorption spectra is multiplied by an imaginary astronomical source spectrum, constant all over the range of wavelength, with three different levels (1, 0.1 and 0.01 mJy), representing a bright, faint and very faint source.

3.1 Ice mixing: major ice species mixed

We add H_2O, CO, CH_3OH and CO alongside the sulfur species. All the band parameters of the chemical species present in the study are extracted from diverse bimolecular mixing with water. When available, we also extracted new band parameters for the sulfur species, mixed with water. The overall composition is discussed and described in Taillard et al, submitted. Considering the shift in position, altered band strength and new vibrational modes available when mixed with water, we look first at the position of the features of the four sulfur species present on the NIR wavelengths. We present in Figure. 1 the position of each of the features of

S-bearing species, with OCS and SO_2 features being relatively isolated while H_2S and CS_2 are overlapping with neighbour features implying the difficulty to identify and detect them.

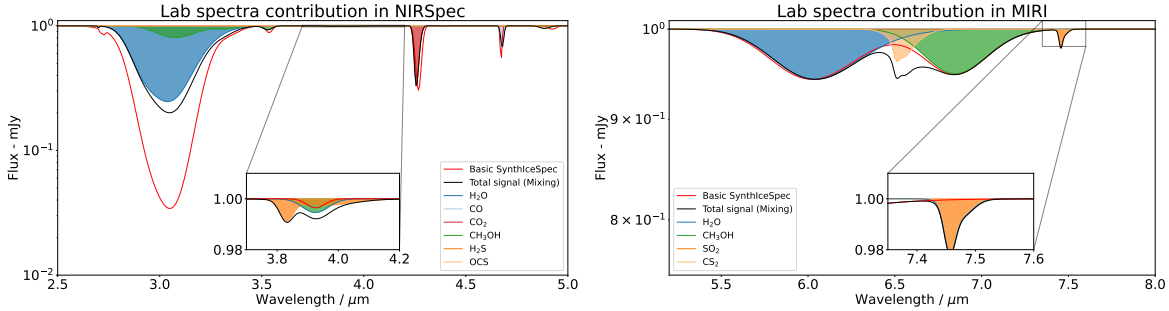

Fig. 1. Synthetic ice spectra of a "simple" ice composition, containing only the major ice species and S-bearing molecules on part of the NIRSpec wavelengths (left) and on a part of the MIRI range (left).

3.2 Model limitations

At the moment, SynthIceSpec lack major features that can impact the overall aspect of the bands such as: grain growth, minor ice features (such as $^{13}CO_2$, dangling O-H, HDO...), ice thermal processing, radiative transfer, mixing (other than with water). The continuum also plays a central role in the column densities determination in real data analysis, that we simplify here with a flat and constant one. It is then expected that the different thresholds we derive are underestimated as compared to what could be observed.

4 Detectability of S-bearing molecules

Now that the positions are known, we test different ice composition, corresponding to data extracted from (Boogert et al. 2015) review. The three ice composition correspond to a cold core, LYSO and MYSO environments. For each case, we iteratively add to the column densities of the four species to reach the values needed for a 5σ detection. We list the different thresholds for each species at each continuum in Table. 1

4.1 H_2S, OCS, SO_2 and CS_2

In each case, the four species are detected with low column densities for a constant flux of 1 mJy, while it gradually gets harder and less realistic as the flux decreases. The ice composition plays a major role in the identification of each species and except OCS that was already detected, the detection of the three other species (H_2S, SO_2 and CS_2) is challenging. A favourable chemistry could help with producing the high and medium flux column densities (at 1 and 0.1 mJy), but no scenario are expected to be reached to form the column densities predicted at 0.01 mJy for all species. Overall, the detection of any of the species listed here would be a milestone, it would benefit the astrochemical models and our comprehension of the sulfur chemistry but as shown in the study, it will remain difficult to constraint the sulfur abundance in the ISM.

4.2 The S_8 case

With the new band parameters for S_8 feature at 21.3 μm, we also tested the column density needed to get a 5σ detection. The band strength being extremely low and distributed on a large band, even with the sulfur cosmic abundance distributed over the allotrope, it would still be impossible to detect the molecule. We computed that we would need almost 10 times the cosmic value to get a 5σ detection.

5 Conclusions

With our study, we showed that the search for identifying the solid sulfur reservoir is difficult with the JWST. We consider a few hypothesis that explain why no major reservoir has been identified so far. Following Fuente et al. (2019) and Cazaux et al. (2022) suggestion of the sulfur being locked on the grains during the translucent

phase and being transformed into S-chains, the detection of the allotropes is simply impossible considering our laboratory data of S_8. Another hypothesis is that sulfur is distributed in ices, so well that the different species column densities are not enough to allow the detection with considered band strength. Then, there might not be a "main" ice reservoir or it is not detectable in the NIR spectrum (for e.g., SH, SO, CS, sulfur salts...).

Table 1. Column densities used in each synthetic spectrum, in parenthesis the abundance relative to water. The 5σ detection thresholds are listed for each S-carrier at each continuum level for all three environments. These thresholds are computed from the rms value derived from McClure et al. (2023).

	Column density (cm^{-2}) (% H_2O)		
Molecule	Cold core	LYSO	MYSO
	(assuming rms level derived from McClure et al. (2023), of 0.003 and 0.005 mJy for NIRSpec and MIRI respectively)		
H_2S (1 mJy)	6.5×10^{16} (0.7%)	1.1×10^{17} (2.2%)	6.5×10^{16} (1.3%)
H_2S (0.10 mJy)	5.1×10^{17} (5.5%)	5.2×10^{17} (10.5%)	4.3×10^{17} (8.6%)
H_2S (0.04 mJy)	9.0×10^{17} (9.7%)	6.6×10^{17} (13.2%)	8.2×10^{17} (16.5%)
OCS (1 mJy)	6.5×10^{15} (0.07%)	5.0×10^{15} (0.1%)	5.0×10^{15} (0.1%)
OCS (0.1 mJy)	1.4×10^{16} (0.15%)	3.0×10^{16} (0.6%)	3.0×10^{16} (0.6%)
OCS (0.04 mJy)	2.8×10^{16} (0.3%)	6.5×10^{16} (1.3%)	6.0×10^{16} (1.2%)
CS_2 (1 mJy)	0.9×10^{16} (0.1%)	1.0×10^{16} (0.2%)	1.0×10^{16} (0.2%)
CS_2 (0.1 mJy)	4.6×10^{16} (0.5%)	4.5×10^{16} (0.9%)	4.5×10^{16} (0.9%)
CS_2 (0.04 mJy)	1.3×10^{17} (1.4%)	1.0×10^{17} (2.0%)	1.1×10^{17} (2.1%)
SO_2 (1 mJy)	1.8×10^{16} (0.2%)	2.5×10^{16} (0.5%)	2.0×10^{16} (0.4%)
SO_2 (0.1 mJy)	1.2×10^{17} (1.3%)	1.5×10^{17} (3.0%)	1.1×10^{16} (2.2%)
SO_2 (0.04 mJy)	2.3×10^{17} (2.5%)	2.6×10^{17} (5.2%)	2.1×10^{17} (4.2%)
S_8	Undetectable assuming all cosmic S abundance locked in the ices		

This work is funded by the European Research Council (ERC) under the Advanced Grant project SUL4LIFE, grant agreement No101096293. A.S.-M. acknowledges support from the RyC2021-032892-I grant funded by MCIN/AEI/10.13039/501100011033 and by the European Union 'Next GenerationEU'/PRTR, as well as the program Unidad de Excelencia María de Maeztu CEX2020-001058-M, and support from the PID2020-117710GB-I00 (MCI-AEI-FEDER, UE). H.C. and G.M.M.C. were funded by project PID2020-118974GB-C21 of the Spanish Ministry of Science and Innovation. R.M.D. was supported by a La Caixa Junior Leader grant under agreement LCF/BQ/PI22/11910030. DNA acknowledges funding support from Fundación Ramón Areces through its international postdoc grant program. AF also thanks project PID2022-137980NB-I00 funded by the Spanish Ministry of Science and Innovation/State Agency of Research MCIN/AEI/ 10.13039/501100011033 and by "ERDF A way of making Europe". J.A.N. and E.D acknowledge support from the French program "Physique et Chimie du Milieu Interstellaire" (PCMI) of the CNRS/INSU with the INC/INP cofunded by the CEA and CNES.

References

Agúndez, M. & Wakelam, V. 2013, Chemical Reviews, 113, 8710

Aikawa, Y., Kamuro, D., Sakon, I., et al. 2012, A&A, 538, A57

Asplund, M., Grevesse, N., Sauval, A. J., & Scott, P. 2009, ARA&A, 47, 481

Boogert, A. C. A., Brewer, K., Brittain, A., & Emerson, K. S. 2022, ApJ, 941, 32

Boogert, A. C. A., Gerakines, P. A., & Whittet, D. C. B. 2015, ARA&A, 53, 541

Calmonte, U., Altwegg, K., Balsiger, H., et al. 2016, Monthly Notices of the Royal Astronomical Society, 462, S253

Cazaux, S., Carrascosa, H., Muñoz Caro, G. M., et al. 2022, A&A, 657, A100

Fuente, A., Navarro, D. G., Caselli, P., et al. 2019, A&A, 624, A105

Fuente, A., Rivière-Marichalar, P., Beitia-Antero, L., et al. 2023, A&A, 670, A114

Gibb, E. L., Whittet, D. C. B., Boogert, A. C. A., & Tielens, A. G. G. M. 2004, ApJS, 151, 35

Jenkins, E. B. 2009, The Astrophysical Journal, 700, 1299

Laas, J. C. & Caselli, P. 2019, A&A, 624, A108

McClure, M. K., Rocha, W. R. M., Pontoppidan, K. M., et al. 2023, Nature Astronomy, 7, 431

Moore, M. H., Hudson, R. L., & Carlson, R. W. 2007, Icarus, 189, 409

Navarro-Almaida, D., Le Gal, R., Fuente, A., et al. 2020, A&A, 637, A39

Palumbo, M. E., Geballe, T. R., & Tielens, A. G. G. M. 1997, ApJ, 479, 839

Palumbo, M. E., Tielens, A. G. G. M., & Tokunaga, A. T. 1995, ApJ, 449, 674
Rocha, W. R. M., van Dishoeck, E. F., Ressler, M. E., et al. 2023, arXiv e-prints, arXiv:2312.06834
Vastel, C., Quénard, D., Le Gal, R., et al. 2018, MNRAS, 478, 5514
Vidal, T. H. G., Loison, J.-C., Jaziri, A. Y., et al. 2017, MNRAS, 469, 435